JOURNAL OF PROPULSION AND POWER
Vol. 23, No. 1, January–February 2007

Magnetohydrodynamic Vortex Containment, Part 2: Equilibrium of Uranium Fluoride Fuel in Hydrogen Propellant

Raymond J. Sedwick* and Daniel A. Zayas†
Massachusetts Institute of Technology, Cambridge, Massachusetts 02139

DOI: 10.2514/1.19711

The second in a series of papers on the effectiveness of using magnetohydrodynamically driven vortices to contain uranium in a gas core nuclear propulsion system is presented. This paper highlights the derivations of equilibrium chemical, electrical, and optical properties that are required to assess the effectiveness of the containment scheme. The primary constituents of the chemical analysis are uranium, hydrogen, and fluorine, and the local thermodynamic equilibrium properties of some 30 of the resulting chemical species are found. Limits on the ability of uranium hexafluoride to reduce condensation of the fuel are presented. Bulk transport properties, including diffusion rates, electrical conductivity, and opacity of the mixture are derived.

Nomenclature

b	=	Debye length
D_{12}	=	H–U diffusion coefficient
d_{12}	=	molecular collision distance
e	=	fundamental charge unit
$G^\circ(T)$	=	Gibbs free energy
g_i	=	degeneracy
h	=	Planck constant
I	=	moment of inertia
I_ν	=	radiative spectral intensity
J	=	rotational quantum number
J_ν	=	spectral emission coefficient
$K_c(T)$	=	equilibrium constant
k	=	Boltzmann constant
m	=	molecular weight
m_e	=	electron mass
n	=	number density
n	=	vibrational quantum number
p	=	pressure
Q	=	partition function
Q_{elec}	=	electrical partition function
Q_{rot}	=	rotational partition function
Q_{tr}	=	translational partition function
Q_{vib}	=	vibrational partition function
$\mathcal{R}$	=	universal ideal gas constant
r	=	radius
$S_{1,2}(T)$	=	Saha equilibrium functions
$S^\circ(T)$	=	standard entropy
T	=	temperature
u	=	radial velocity
V	=	volume
x	=	mole fraction
y	=	mass fraction
α	=	Lagrange multiplier
$\Delta_{\text{aff}}\text{H}^\circ$	=	electron affinity
$\Delta_d\text{H}^\circ$	=	enthalpy of dissociation
$\Delta_f\text{H}^\circ$	=	enthalpy of formation
$\Delta_i\text{H}^\circ$	=	heat of ionization
ϵ_i	=	energy level i
θ_v	=	vibrational temperature
θ_{rot}	=	rotational temperature
κ_ν	=	spectral absorption coefficient
κ_R	=	Rosseland mean opacity
λ_R	=	radiative conduction coefficient
μ	=	chemical potential
ν	=	vibrational frequency
$\bar{\nu}_e$	=	collision frequency
ν_i	=	stoichiometric coefficients
ρ	=	density
σ	=	conductivity
τ_ν	=	optical depth
$\phi^\circ(T)$	=	Gibbs function

Received 29 August 2005; revision received 10 April 2006; accepted for publication 31 May 2006.

*Principal Research Scientist, Space Systems Laboratory, Department of Aeronautics Astronautics; sedwick@mit.edu. AIAA Senior Member.

†Graduate Research Fellow, Space Systems Laboratory, Department of Aeronautics Astronautics. AIAA Member.

Introduction

IF manned missions to Mars or beyond are to become feasible, it will be necessary to develop very high-power-density propulsion systems. Present-day chemical propulsion concepts, although capable of the thrusts required for short transfer times, are incapable of producing the high specific impulses necessary to achieve reasonable fuel–payload ratios. Various power systems including nuclear fission, nuclear fusion and even matter–antimatter annihilation are theoretically capable of generating the necessary power densities, yet only nuclear fission systems have been adequately developed beyond mere proof of concept. Such systems use the heat generated from a uranium fission reaction to increase the internal energy of a gaseous propellant, such as hydrogen, before expanding it through a nozzle. This direct conversion from thermal to kinetic energy results in a higher specific impulse, but is limited by the melting points of the fuel and reactor assembly. One way to exceed such limitations is the implementation of liquid or gaseous fuel injection, allowing the system to operate at significantly higher temperatures. The use of fuels in the gas phase poses the unique challenge of confining the fuel until it is consumed by the reaction, while effectively transferring the reaction energy to the propellant and isolating the reactor assembly from the high propellant temperatures that result.

As discussed in the first paper of this series [1], one early containment scheme developed by Kerrebrock and Meghreblian [2] considered the use of a hydrodynamic vortex to establish a pressure gradient within a cylindrical cavity. This gradient could push propellant through a heavy fissile fuel, while at the same time keeping the fuel isolated from the walls of the cavity. Although

originally promising, this approach was deemed unworkable due to the fact that the coupling of the vortex strength to the mass flow rate would not allow sufficient containment, regardless of injection velocity. To decouple these effects, the idea of using magneto-hydrodynamic forces to strengthen the vortex was pursued. A summary of the results can be found in the overview paper [1], with a greater level of detail found in the project final report [3]. The effectiveness of the containment scheme required a detailed evaluation of the fluid, electrical and optical transport properties of the flow, which, in turn, required the chemical composition of the system across a large variation in pressures, temperatures, and constituent concentrations to be evaluated. The following details the development of the equilibrium concentrations and the resulting transport properties.

Uranium Condensation

To provide a more complete treatment of the transport properties, including diffusion and conductivity, the chemical state needs to be determined throughout the flow. One of the performance features demonstrated by Kerrebrock and Meghreblian [2] was a significant drop in engine mass as the uranium loading was increased. This was due to a reduction in the critical mass by increasing the fission probability. One way to increase this loading is to increase the ratio of fuel to propellant w. The other way is to increase the overall density (and hence pressure) of the propellant–fuel combination, which may be taken as high as the pump technology and structural limitations will allow. The results presented for the original design assumed a pressure level of 100 atm to achieve the reported thrust-to-weight ratios. With current pump technology, such as the high-pressure fuel turbopump of the space shuttle main engine, pressure levels of 460 atm at flow rates of 70 kg/s can be achieved [4].

One problem that develops when such high pressures are generated is that the vapor pressure of metallic uranium is not high enough to maintain a gas phase. The difficulty of uranium condensation is not unique to the open-cycle vortex containment system, as all gas core engines achieve greater performance (lower mass) when a higher level of uranium loading is present. However, because containment in this system relies on diffusion (resulting from a balance of high-pressure gradients and centrifugal accelerations) the partial pressure and mean particle size of the uranium is key to determining how the fuel will be distributed through the system and whether, upon condensing out of the gas phase, it will accumulate at the vortex wall.

Over the years, the vapor pressure problem has been addressed by suggesting that the uranium be introduced as a fluoride (UF_6, UF_4), which has a much higher vapor pressure than metallic uranium. However, because hydrogen (the propellant of choice due to its low molecular weight) is so highly reactive with the halides, it has a tendency to reduce the fluoride compounds by producing hydrogen fluoride (HF). The large particle-density ratio of hydrogen to uranium also suggests that there will be no shortage of hydrogen available to supply this reaction. One important question that must therefore be answered is to what extent compounds of uranium fluoride can be maintained in the presence of hydrogen.

The use of fluorinated uranium also poses several other complications. For example, it will be necessary to determine the electrical properties of this mixture of hydrogen, uranium, and fluorine, so that the effectiveness of applying the electromagnetic field to strengthen the vortex can be determined. To help answer these questions, the species that will be included in the analysis are H_2, H, H^+, H^-, F_2, F, F^+, F^-, HF, U, U^+, and e^- and all neutrals, anions, and cations of UF_6 through UF (30 species in all). Because of the high number densities and collision rates, it will be assumed for this analysis that the gas is in a state of local thermodynamic equilibrium (LTE), so that the equilibrium constants for composition and ionization will be determined from the partition functions of each species.

Finally, the optical properties of the gas mixture must be investigated to determine the contribution of radiative heat transfer to redistribution of energy through the system. Because of the high temperatures that are sought at the core of the vortex, the potential exists for the unrestricted transfer of radiative energy across the vortex to the wall. This would generate a direct state of thermodynamic equilibrium between the core and the wall, eliminating the possibility of maintaining an elevated core temperature. By determining the optical depth of the gas mixture, a lower limit can be placed on the dimensions of the vortex tube, hence the feasibility of constructing a useful matrix of these tubes can be determined.

General Partition Functions

Following the methodology of [5,6], Boltzmann statistics defines the number of particles in the $Q3$ energy level (with degeneracy) as

$$N_i = g_i \exp\left[\frac{\alpha - \epsilon_i}{kT}\right] \tag{1}$$

where α is used to impose a given total number of particles when maximizing the overall statistical weight.

Summing for all energy levels,

$$N = \sum_i g_i \exp\left[\frac{\alpha - \epsilon_i}{kT}\right] = \exp\left[\frac{\alpha}{kT}\right] \sum_i g_i \exp\left[\frac{-\epsilon_i}{kT}\right] \tag{2}$$

where the final summation is defined as the partition function (PF).

Dividing Eq. (1) by Eq. (2)

$$\frac{N_i}{N} = \frac{g_i \exp[-\epsilon/kT]}{Q} \tag{3}$$

gives the partition of particles among energy levels, as the fraction contributed by each level to Q. In the summation $\sum_i$, i represents an energy level. Because g_i is the number of quantum states that all have the same energy, the sum can be written instead over quantum states, omitting g_i, as

$$Q = \sum_{\text{states}} \exp[-\epsilon_i/kT] \tag{4}$$

For noninteracting degrees of freedom, ϵ_i is decomposable as

$$\epsilon_i = \epsilon_i^{\text{tr}} + \epsilon_i^{\text{rot}} + \epsilon_i^{\text{vib}} + \epsilon_i^{\text{elec}} \tag{5}$$

and the partition function can be separated as follows

$$Q = \sum_{\text{states}} e^{-\frac{\epsilon_i^{\text{tr}}}{kT}} e^{-\frac{\epsilon_i^{\text{rot}}}{kT}} e^{-\frac{\epsilon_i^{\text{vib}}}{kT}} e^{-\frac{\epsilon_i^{\text{elec}}}{kT}} \ldots = \left(\sum_{\text{tr}} e^{-\frac{\epsilon_i^{\text{tr}}}{kT}}\right)\left(\sum_{\text{rot}} e^{-\frac{\epsilon_i^{\text{rot}}}{kT}}\right)\ldots \tag{6}$$

or written as

$$Q = Q_{\text{tr}} Q_{\text{rot}} Q_{\text{vib}} Q_{\text{elec}} \tag{7}$$

with partition functions representative of translation, rotation, vibration, and electron configuration, respectively. To determine the form of each partition function, the energy and degeneracy associated with each component of energy must be found.

For translation, the energy is the kinetic energy of the particle, which, classically, can take on any value. A quantum mechanical treatment of the translation, however, relates the allowable kinetic energies of a particle to the wave functions for which an integer number of half-waves may be contained in a box of some arbitrary size. In this way, the translational partition function represents the number of boxes with size of the de Broglie wavelength in a given volume. Each energy state is represented by

$$\epsilon_{s_x s_y s_z} = \frac{h^2}{8m}\left(\frac{s_x^2}{L_x^2} + \frac{s_y^2}{L_y^2} + \frac{s_z^2}{L_z^2}\right) \tag{8}$$

where s_x, s_y, and s_z are the integral quantum numbers, and L_x, L_y, and L_z are the dimensions of the box. To calculate the PF summation, the harmonics are approximated to represent a continuum of states, and the sum is taken as an integral that has the form of a Gaussian.

The resulting translational partition function is given by

$$Q_{\text{tr}} = \left(\frac{2\pi mkT}{h^2}\right)^{3/2} V \tag{9}$$

where $V = L_x L_y L_z$ is the volume of the box.

The vibrational PF comes from approximating each normal mode of oscillation by a harmonic oscillator, and the quantum mechanical energy for the vibrational quantum number of that mode is given by

$$\epsilon_n = h\nu\left(n + \frac{1}{2}\right) \tag{10}$$

Assuming singly degenerate modes, the PF can be written as

$$Q_{\text{vib}} = \sum_{n=0}^{\infty} \exp\left[-\frac{h\nu[n + (1/2)]}{kT}\right] \tag{11}$$

which, after pulling out the common factor corresponding to the zero point energy, leaves

$$\sum_{n=0}^{\infty}\left(\exp\left[-\frac{h\nu}{kT}\right]\right)^n = \frac{1}{1 - \exp[-(h\nu/kT)]} \tag{12}$$

The combination $h\nu/k$ is defined as the characteristic vibrational temperature, giving as the final form

$$Q_{\text{vib}} = \frac{\exp[-\theta_v/2T]}{1 - \exp[-\theta_v/T]} \tag{13}$$

The energy associated with the quantum number of a rotational mode is

$$\epsilon_J = \frac{h^2 J(J+1)}{2I} \tag{14}$$

and the degeneracy is $g_J = 2J + 1$. Approximating the summation over J as an integral over a continuum of values, a similar result to that of the translational PF is obtained. For diatomic (or linear polyatomic) molecules, the result is

$$Q_{\text{rot}} = \frac{8\pi^2 IkT}{\sigma h^2} = \frac{T}{\sigma\theta_{\text{rot}}} \tag{15}$$

and for nonlinear polyatomic molecules, the result is

$$Q_{\text{rot}} = \frac{1}{\sigma}\left(\frac{\pi T^3}{\theta_{r1}\theta_{r2}\theta_{r3}}\right)^{1/2} \tag{16}$$

where $\sigma = 1$ for asymmetric and $\sigma = 2$ for symmetric molecules, to account for the double counting of identical states.

Finally, the electronic partition function (with energy referenced from the ground state configuration) is represented by a summation of energy levels with known degeneracies as

$$Q_{\text{elec}} = g_\circ + \sum_{i=1}^{\infty} g_i \exp[-\epsilon_i/kT] \tag{17}$$

Because the jump from the ground state to the first excited state is often quite large (levels then get closer together as n increases), it is often sufficient to approximate this partition function by simply using the ground state degeneracy $g_\circ$. As the temperature approaches a significant fraction of the energy of the first excited state (above 10,000 K), however, the contribution of these higher energy states must be included.

Hydrogen, Fluorine, and Electrons

The diatomic, monatomic, and ionic partition functions between hydrogen and fluorine are very similar in form. For the diatomic molecules, the partition function is the product of the translation, vibration, rotation, and electronic functions and can be written per unit volume as follows:

Table 1 Parameters of diatomic partition functions

	$g_\circ$	σ	θ_v, K	θ_r, K	θ_d, K	m_{xy}/m_h
H_2	1	2	6100	85.4	51968	2
HF	1	1	3713	6.33	32870	20
F_2	1	2	2260	0.0292	37180	38

$$q_{xy} = \left(\frac{Q_{\text{tr}}}{V}\right) Q_{\text{vib}} Q_{\text{rot}} Q_{\text{elec}} \tag{18}$$

or, in terms of the previously derived formulas, as

$$q_{xy} = g_\circ\left(\frac{2\pi m_{xy}kT}{h^2}\right)^{3/2}\left(\frac{T}{\sigma\theta_{\text{rot}}}\right)\left(\frac{\exp[-\theta_v/2T]}{1 - \exp[-\theta_v/T]}\right)\exp[-\Delta/T] \tag{19}$$

where the constants in this formula for the various species are given in Table 1 [7,8]. It will be shown that the Δ will act as an arbitrary shift in the energy to allow the proper value of enthalpy to be set relative to the reference temperature.

The reference temperature at which the natural state of the element is set to zero enthalpy is taken as 0 K to be consistent with the enthalpy formulas (given shortly) for the uranium fluorides. To achieve this, the enthalpy is calculated from the partition function of the species by the relation

$$h = \mathcal{R}T^2 \frac{\partial \ell_n\, q}{\partial T} + \mathcal{R}T \tag{20}$$

where the enthalpy is given in J/mol · K. For the diatomic species, this yields

$$\frac{h}{\mathcal{R}} = \frac{7}{2}T + \left(\frac{\theta_v}{2} + \Delta\right) + \frac{\theta_v}{1 - \exp[-\theta_v/T]} \tag{21}$$

and for H_2 and F_2, setting $h(0) = 0$ yields $\Delta = -\theta_v/2$. This effectively subtracts from the zero point contribution of the harmonic oscillator. For HF, the enthalpy balance at 0 K must be consistent with the formula for its creation from its diatomic constituents:

$$h_{H_2}(0) + h_{F_2}(0) = 2h_{\text{HF}}(0) - 2\Delta_f \text{H}^\circ(0) \tag{22}$$

and, therefore, the value of Δ is found from

$$\frac{h_{\text{HF}}(0)}{\mathcal{R}} = \frac{\theta_v}{2} + \Delta = \frac{\Delta_f \text{H}^\circ(0)}{\mathcal{R}} = \theta_d \tag{23}$$

where the characteristic dissociation temperature is given in Table 1.

For the monatomic species of H and F, as well as for the electrons, the only degrees of freedom are translational and electronic, and the general form of the partition function is

$$q_x = g_\circ\left(\frac{2\pi m_x kT}{h^2}\right)^{3/2} \exp[-\Delta/T] \tag{24}$$

where, once again, the Δ allows for a shift in the reference energy, and $g_\circ$ is used to approximate the electronic PF. Applying Eq. (20) to this form of the partition function gives enthalpy in the form

$$\frac{h}{\mathcal{R}} = \frac{5}{2}T + \Delta \tag{25}$$

The enthalpies for H and F must also be consistent with their formation energies from the respective diatomic species. Hence,

$$h_{x_2}(0) + \Delta_d \text{H}^\circ(0) = 2h_x(0) \tag{26}$$

where $\Delta_d \text{H}^\circ$ has been introduced as the energy of dissociation per mole, and is related to the characteristic temperature of dissociation by $\Delta_d \text{H}^\circ = \mathcal{R}\theta_d$. The partition functions for H and F are, therefore,

$$q_{\mathrm{H}} = 2\left(\frac{2\pi m_{\mathrm{H}} kT}{h^2}\right)^{3/2} \exp[-\theta_{d\mathrm{H}}/2T] \tag{27}$$

$$q_{\mathrm{F}} = 6\left(\frac{2\pi m_{\mathrm{F}} kT}{h^2}\right)^{3/2} \exp[-\theta_{d\mathrm{F}}/2T] \tag{28}$$

where the degeneracy of hydrogen represents the two possible electron spin states at ground level, and the degeneracy of fluorine is an effective value that includes states with energies less than 0.2 eV above the ground level [5]. Because the electrons come from and join to various sources, the characteristic temperatures of ionization will be attached to the parent molecule instead of the electron, in much the same way that the dissociation energy can be attached to either the diatomic or monatomic species. The Δ value for the electron partition function is therefore set to zero, and the degeneracy is two ($g_\circ = 2$), to account for each spin state.

For the ionized states of H and F (both anion and cation), the partition functions are very similar in form to those for the atomic species, with different values for the energy offset and degeneracy. Both ionized states of hydrogen and the anion of fluorine (F^-) have a degeneracy of one because the highest populated set of orbitals is full. For the cation of fluorine, the degeneracy is approximately nine, where, once again, the energy states close to the ground state have been included [5]. The enthalpy balance for the cations has the form

$$h_x(0) + \Delta_{x_i}\mathrm{H}^\circ(0) = h_{x^+}(0) + h_e(0) \tag{29}$$

and for the anions

$$h_x(0) + h_e(0) = h_{x^-}(0) + \Delta_{x_{\mathrm{aff}}}\mathrm{H}^\circ(0) \tag{30}$$

The energies of ionization ($\Delta_{x_i}\mathrm{H}^\circ$) and electron affinity ($\Delta_{x_{\mathrm{aff}}}\mathrm{H}^\circ$) are related to their characteristic temperatures in the same way as the energies of formation and dissociation, with the resulting formulas for the PFs written as

$$\begin{aligned}
q_{\mathrm{H}^+} &= \left(\frac{2\pi m_{\mathrm{H}} kT}{h^2}\right)^{3/2} \exp\left[\frac{-\theta_{d\mathrm{H}_2}/2 - \theta_{\mathrm{H}_i}}{T}\right] \\
q_{\mathrm{H}^-} &= \left(\frac{2\pi m_{\mathrm{H}} kT}{h^2}\right)^{3/2} \exp\left[\frac{-\theta_{d\mathrm{H}_2}/2 + \theta_{\mathrm{H}_{\mathrm{aff}}}}{T}\right] \\
q_{\mathrm{F}^+} &= 9\left(\frac{2\pi m_{\mathrm{F}} kT}{h^2}\right)^{3/2} \exp\left[\frac{-\theta_{d\mathrm{F}_2}/2 - \theta_{\mathrm{F}_i}}{T}\right] \\
q_{\mathrm{F}^-} &= \left(\frac{2\pi m_{\mathrm{F}} kT}{h^2}\right)^{3/2} \exp\left[\frac{-\theta_{d\mathrm{F}_2}/2 + \theta_{\mathrm{F}_{\mathrm{aff}}}}{T}\right]
\end{aligned} \tag{31}$$

where the values of the ionization energy and electron affinity for H and F are [5]

$$\begin{gathered}
\theta_{\mathrm{H}_i} = 158,000\ \mathrm{K} \qquad \theta_{\mathrm{H}_{\mathrm{aff}}} = 9,000\ \mathrm{K} \qquad \theta_{\mathrm{F}_i} = 202,000\ \mathrm{K} \\
\theta_{\mathrm{F}_{\mathrm{aff}}} = 42,000\ \mathrm{K}
\end{gathered} \tag{32}$$

Uranium Fluorides

Because of the large number of electron energy levels in compounds of uranium and fluorine, it is not sufficient to approximate the electronic contribution to the partition function as the ground state degeneracy. It is also not convenient to represent the function as a large sum of exponentials, one for each independent energy value. Instead, Gurvich, et al. [9] generated, from both experimental and theoretical data, a set of curve fits to the Gibbs function $\phi^\circ(T)$, from which all thermodynamic properties of the gaseous U–F systems can be calculated. The Gibbs function is defined as

$$\phi^\circ(T) = -\frac{G^\circ(T) - \Delta\mathrm{H}_f{}^\circ(0)}{T} \tag{33}$$

and the functional form of the curve fit is given as

$$\phi^\circ(T) = \phi_0 + \phi\,\ell n\, x + \frac{\phi_{-2}}{x^2} + \frac{\phi_{-1}}{x} + \phi_1 x + \phi_2 x^2 + \phi_3 x^3 \tag{34}$$

where $x = T/(10^4\ \mathrm{K})$, and the units of ϕ° are $\mathrm{J/mol \cdot K}$. The temperature range of validity for this equation is between 1000 and 10,000 K, and the values for the anions, cations, and neutrals of UF_n are tabulated in Table A1 for $n = 0$ to 6. The heats of formation for these molecules at 0 K ($\Delta_f\mathrm{H}^\circ(0)$) are also listed.

The Gibbs function defined here is related to the standard entropy, which can be seen by writing the expression for $\phi^\circ(T)$ as

$$\begin{aligned}
\phi^\circ(T) &= -\frac{G^\circ(T) - \mathrm{H}^\circ(T) + [\mathrm{H}^\circ(T) - \mathrm{H}^\circ(0)]}{T} \\
&= S^\circ(T) - \frac{\mathrm{H}^\circ(T) - \mathrm{H}^\circ(0)}{T}
\end{aligned} \tag{35}$$

where the standard entropy $S^\circ(T)$ is evaluated at standard pressure (1 atm).

To relate the Gibbs function to the partition function, the Gibbs free energy at standard pressure is given as

$$G^\circ = -\mathcal{R}T\,\ell n(Q/N)^\circ \tag{36}$$

where the ratio Q/N can be written equivalently as q/n by dividing the volume out of both Q and N. Rearranging in terms of the partition function yields

$$q = \frac{p^\circ}{kT}\exp\left\{\frac{\phi^\circ}{\mathcal{R}} - \frac{\Delta_f\mathrm{H}^\circ(0)}{\mathcal{R}T}\right\} \tag{37}$$

with the reference pressure taken as 1 atm. It should be noted that the ideal gas constant is used in the exponential of Eq. (37) because the Gibbs function is expressed "per mole," whereas the Boltzmann constant is used to specify the partition function in a manner suited to particle densities. Applying Eq. (20) to calculate the enthalpy gives the relationship

$$h = \frac{\mathrm{d}\phi^\circ}{\mathrm{d}T}T^2 + \Delta_f\mathrm{H}^\circ(0) \tag{38}$$

which can be differentiated further to obtain the specific heat at constant pressure.

Chemical and Saha Equilibrium

Now that the partition functions for each of the species have been developed, they can be combined to determine the equilibrium composition and ionization of the gas mixture. A general equilibrium chemical reaction can be represented algebraically in the form

$$\sum \nu_i A_i = 0 \tag{39}$$

where A_i represents the species and ν_i are taken as positive for products and negative for reactants. The condition for chemical equilibrium can then be written

$$\sum \nu_i \mu_i = 0 \tag{40}$$

which states that the sum of the chemical potentials (weighted by the stoichiometric coefficients) for all species must equal zero. Writing the chemical potential in terms of the partition function yields

$$\mu = -kT\,\ell n(q/n) \tag{41}$$

and the expression for equilibrium becomes

$$-kT\sum \nu_i\,\ell n\left(\frac{q}{n}\right) = 0 \tag{42}$$

Finally, exponentiating both sides of the equation and separating the number densities from the partition functions gives

$$\prod (n_i)^{\nu_i} = \prod (q_i)^{\nu_i} = K_c(T) \tag{43}$$

The same analysis can be applied in the case of ionization. The reactions that occur are either that of the addition or removal of an electron, represented by $X + e^- \rightleftharpoons X^-$ or $X \rightleftharpoons X^+ + e^-$, respectively. Because the energy levels of the ions have already been properly referenced to their associated neutrals, the number densities of the reacting species can be related in the same manner as previously shown, to yield

$$\frac{n_\circ n_e}{n_-} = \frac{q_\circ q_e}{q_-} = S_1(T) \qquad \frac{n_+ n_e}{n_\circ} = \frac{q_+ q_e}{q_\circ} = S_2(T) \tag{44}$$

To solve for the concentrations of all the chemical and ionic species, an iterative procedure was used. The inputs to the procedure are the total pressure and temperature of the gas and the total number of uranium and fluorine atoms (presented as fractions of the number of hydrogen atoms). The maximum possible number of hydrogen atoms present is first estimated assuming that diatomic hydrogen is the only species ($n_{H_2} = p/kT$). The number of atoms of uranium and fluorine present are then calculated from the specified fractions, and the equilibrium constants are evaluated from the previous formulas. The concentrations of each species are estimated from the equilibrium constants, and the resulting pressure is calculated from the temperature and total particle density. The process continues iteratively until the final pressure of the system is equal to what was originally specified. The same method is used to determine the equilibrium ionization state by estimating the value of the electron number density and using the Saha functions to then calculate the anion and cation populations. This results in a new estimate for the electron population, and the iteration continues until convergence.

Figures 1 and 2 show the mole fractions of the species present from 2000 to 10,000 K, as low as 10^{-7}. Figure 1 has a uranium mass fraction of 18%, corresponding to the uranium loading for a subcritical heating value at the outer wall of the vortex. The number of fluorine atoms present is set to six times the uranium atoms, corresponding to the uranium being present as UF_6. At injection temperatures around 2500–3000 K, the populations of the higher fluorides of uranium have already been nearly eliminated by the formation of HF. The most abundant form of uranium at 3000 K is UF_2, which is present in concentrations three orders of magnitude above the metallic uranium. The vapor pressure line of metallic uranium has been included on the graph by displaying the mole fraction calculated from the ratio of vapor to total pressure (at 100 atm). Comparison to the actual mole fraction of metallic uranium present shows that, at this level of fluorination, the metallic uranium content has been suppressed to the point that condensation will not occur. This is demonstrated by the fact that the partial pressure (shown as a mole fraction) of metallic uranium is below its vapor pressure. However, as the amount of fluorine in the system is reduced, the partial pressure of metallic uranium will rise above the vapor pressure line, indicating that condensation will occur. This situation is shown in Fig. 2, where the number of fluorine atoms has been reduced by an order of magnitude and the same amount of uranium is present, effectively reducing the mass fraction of fluorine by 7%.

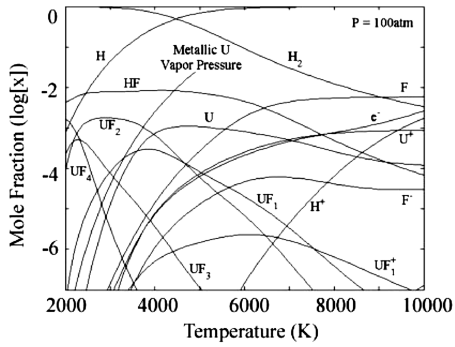

Fig. 1 Mole fractions of the H–UF_6 system (74, 18, and 8% by mass).

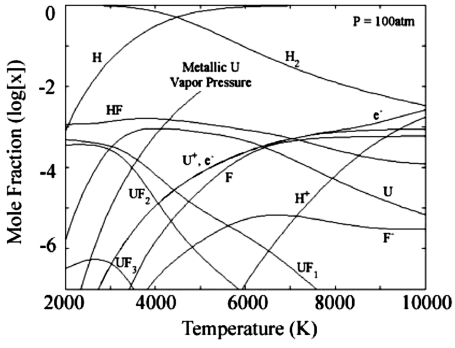

Fig. 2 Mole fractions of the H–U–F system (80, 19, and 1% by mass).

Because the fuel consumption (and hence replenishment) rate is small compared with the propellant usage, the fluorine will also enter the vortex at a comparatively low rate (as UF_6). The vortex is designed to support a uranium distribution and, therefore, free fluorine (or HF) cannot be contained within the vortex because its molecular mass is only 1/10 that of the uranium. This can be seen from the equation for the diffusion velocity:

$$u_2 = -D_{12}\frac{\rho_1}{\rho}\left[\frac{n}{n-n_2}\frac{\mathrm{d}\log(n_2/n)}{\mathrm{d}r} + \frac{n(m_1-m_2)}{\rho}\frac{\mathrm{d}\log p}{\mathrm{d}r}\right] \tag{45}$$

To maintain position within the vortex, the uranium must diffuse outward so that its relative velocity is equal and opposite to that of the hydrogen flow. The fluorine must therefore achieve the same diffusion velocity to stay in the vortex. The diffusion coefficient (discussed later) between F and H as compared with U and H differs only slightly due to a difference in the reduced molecular weights, but mostly in the collision diameter. Basing the collision diameter of each pair on the sum of their van der Waals radii, the two diffusion coefficients are the same to within 10%. Assuming that the number density of the fluorine is significantly smaller than that of the hydrogen (as with the uranium), the statement of equal diffusion velocities reduces to the requirement

$$\frac{\mathrm{d}\log n_\mathrm{U}}{\mathrm{d}r} - \frac{\mathrm{d}\log n_\mathrm{F}}{\mathrm{d}r} = (m_\mathrm{U} - m_\mathrm{F})\frac{n}{\rho}\frac{\mathrm{d}\log p}{\mathrm{d}r} \tag{46}$$

and near the core, where $\rho \sim n_\mathrm{H} m_\mathrm{H}$, the coefficient of the log p term is approximately constant. The resulting equation can be written

$$\frac{n_\mathrm{U}}{n_\mathrm{F}} = \frac{1}{6}\left(\frac{p}{p_c}\right)^{\left(\frac{m_\mathrm{U}-m_\mathrm{F}}{m_\mathrm{H}}\right)} \tag{47}$$

where it has been assumed that in steady-state operation, the particle flow rate of the fluorine is six times that of the uranium (because it is introduced as UF_6) at the core of the vortex. Because of the very large exponent on the pressure ratio, the number density of the fluorine must actually drop with increasing radius. This makes physical sense, in that the reduced pressure diffusion rate (due to lower molecular mass) must be compensated for by a negative concentration gradient. However, a massive reduction in number density from this already low value means that no fluorine can be maintained in the vortex and, for the remaining analysis of the vortex region, the fluorine will be neglected.

One area where the fluorination of the uranium will have a marked effect is in the injection of uranium into the system. It must be carried by feeds from the storage area and, consequently, must be maintained in the gas phase. The question arises as to whether the fuel can be carried to the vortex chambers in the same feed tubes as the hydrogen, or must be piped in separately to avoid reduction to metallic uranium by the propellant. Within the feed tubes, the problem of differential pressure diffusion is not present, and the relative concentrations of fuel and propellant are governed by the two mass flow rates. Operationally, the mass flow rate of the uranium will be determined by the power level of the reactor and the rate at which the uranium in consumed (and hence replenished). As the power level is dependent on many system-level issues that have not at this

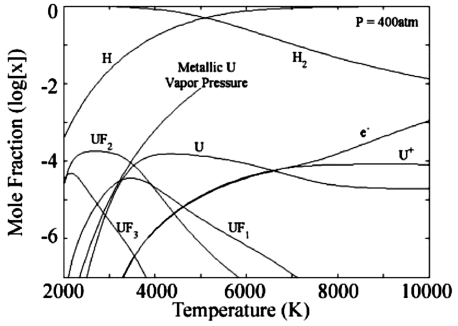

Fig. 3 Mole fractions of H–U–F system (97, 2, and 1% by mass).

point been addressed, the condition on the fuel mass flow rate is set by establishing a loss rate that is low enough to keep the reduction in specific impulse below 1%. This same condition set $\mathcal{M}_2/\mathcal{M}_1$ to 10^{-4} in the previous work.

Figure 3 shows this mass fraction (2%) of uranium, with a fluorination level consistent with it having been introduced as UF_6 (mass fraction of 1%). The pressure level was set to 400 atm, under the assumption that the flow would not at this point have passed through the injectors (the vapor pressure line of metallic uranium is again shown for reference). It is seen that condensation of uranium is again suppressed by pushing the partial pressure of the metallic uranium below its vapor pressure line. If it is determined that the supply rate of fuel should be changed to another value (due to power replenishment considerations) and the partial pressure rises above the condensation line, the problem could be easily alleviated by injecting a small amount of fluorine into the system in addition to what is carried in by the uranium. At this rate of uranium flow, a significant amount of fluorine could be introduced, if necessary, without adversely affecting the specific impulse. Thus, the fuel can be fed to the vortices along with the propellant. This is a great advantage, as otherwise some inert buffer gas would be needed to carry the gaseous uranium along a second set of feed tubes, adding complexity to the system and reducing the specific impulse. Although fission may occur in the feed tubes, the replenishment rate is so small that only trace amounts of uranium are present, making the power generated very small.

Bulk Transport Properties

In light of the full chemical analysis of the previous section, the dominant chemical species are now identified as U, U^+, H_2, H, H^+, and e^-. For future analysis of the fluid mechanics of the system, it will be necessary to develop expressions for the effective specific heat, diffusion characteristics, and conductivity of the mixture. The gas flow will be modeled as three fluids: hydrogen, uranium, and electrons. Within each fluid, the chemical properties of its constituents will be averaged to achieve a single set of effective characteristics. This implies that molecules of H_2, H, and H^+ are not assumed to diffuse differentially and neither are U and U^+. The assumption is also made that the high collisionality will allow the electron temperature and the heavy species temperature to be the same.

Specific Heat

The heat convection through the system will require an expression for the mass-averaged enthalpy of the gas as a function of temperature. In fact, it is the derivative of the enthalpy with temperature (the specific heat at constant pressure) that will appear explicitly in the formulation. From the expression for the enthalpy of diatomic hydrogen

$$\frac{h}{\mathcal{R}} = \frac{7}{2}T + \frac{\theta_v}{1-\exp[-\theta_v/T]} \tag{48}$$

the specific heat per unit mass (c_p) is found by differentiating and dividing by the molecular weight ($m_{H_2} = 2$), leaving

$$c_p = \left[\frac{7}{2} + \frac{(\theta_v/T)^2 \exp[-\theta_v/T]}{(1-\exp[-\theta_v/T])^2}\right]\frac{\mathcal{R}}{2} \tag{49}$$

which can be simplified in terms of the hyperbolic sine function as

$$c_p = \left[\frac{7}{2} + \left(\frac{\theta_v/2T}{\sin h(\theta_v/2T)}\right)^2\right]\frac{\mathcal{R}}{2} \tag{50}$$

For both the hydrogen atom and the hydrogen ion, the only variation of the enthalpy with temperature is due to the translational motion and, with a molecular weight of $m = 1$, the specific heat for both is $c_p = \frac{5}{2}\mathcal{R}$. To determine the mass-averaged specific heat, the mole fraction of n_H is first determined from the equilibrium relationship

$$\frac{n_H^2}{n_{H_2}} = K_c \tag{51}$$

by dividing through by the total particle density and rewriting the LHS in terms of $n_H/n = x$ as follows

$$\frac{(n_H/n)^2}{1-(n_H/n)^2} = \frac{x^2}{1-x} = K_c/n = K_n \tag{52}$$

Solving for the mole fraction then gives

$$x = 1/2[(K_n^2 + 4K_n)^{1/2} - K_n] \tag{53}$$

The mass fraction is defined as

$$y = \frac{\rho_H}{\rho_H + \rho_{H_2}} = \frac{n_H}{n_H + 2n_{H_2}} \tag{54}$$

which can be written in terms of the mole fraction as

$$y = x/(2-x) \tag{55}$$

The mass-averaged specific heat can finally be written as

$$\frac{dh_H}{dT} = yc_{p_0} + (1-y)c_{p_1} \tag{56}$$

where c_{p_0} is the specific heat per unit mass of n_H (neutrals and ions) and c_{p_1} is the specific heat per unit mass of n_{H_2}. The mass specific heat of both the electrons and the uranium, although similar in form, are not worthy of further analysis, as in both cases the mass flow rate is too small to carry a significant portion of the heat through the system.

Binary Diffusion Coefficient

In treating the diffusion of the hydrogen propellant through the uranium fuel, it is necessary to determine the diffusion coefficient. Although five heavy species are considered (two uranium, three hydrogen), the properties of each family are averaged, and a single binary diffusion coefficient is identified between them. For neutral particles the interaction may, without significantly sacrificing accuracy, be modeled as a collision between rigid elastic spherical molecules that do not have a field of force. Evaluation of the collision integral for hard sphere collisions gives for the binary diffusion coefficient [10]

$$D_{12} = \frac{3}{8nd_{12}^2}\left[\frac{(m_1+m_2)\mathcal{R}T}{2\pi m_1 m_2}\right]^{1/2} \tag{57}$$

where m_1 and m_2 are in g/mol and d_{12} is the diameter of the collision cross section (sum of the particle radii). As both the uranium fuel and hydrogen propellant ionize, the collision cross section between the two ionized species will increase due to the Coulomb repulsion. Although the force field of a given ion reaches infinitely far, the presence of the electrons (quasi-neutrality) will tend to shield the repulsive forces of the ions, generating an equivalent finite collision cross section between them. This cross section is related to the Debye length of the mixture, and evaluation of the collision integral for the inverse square law force yields [10]

$$D_{12}^{+} = D_{12} d_{12}^2 \frac{q^2}{\ell_n[1 + (2bq)^2]} \tag{58}$$

where b is given as

$$b = \left(\frac{\epsilon_0 kT}{n_e e^2}\right)^{1/2} \tag{59}$$

and q is defined as

$$q = \left(\frac{8\pi\epsilon_0 kT}{e^2}\right) \tag{60}$$

As a check, in the limit as the number density of the electrons (ions) becomes large, the product $(2bq)^2$ will be small compared with one, and the natural log term will be approximately equal to $(2bq)^2$. The expression then reduces to

$$D_{12}^{+} = D_{12} \frac{d_{12}^2}{(2b)^2} \tag{61}$$

where, effectively, the hard sphere collision diameter is replaced by twice the Debye length, which is equivalent to the charged particle collision diameter.

Returning to the equilibrium composition analysis, it can be seen in Fig. 1 that even at temperatures as high as 10,000 K, the ionization fraction of the hydrogen is only 10^{-3}, so that binary diffusion based on Coulomb repulsion does not come into play. Between 7000 and 10,000 K, the uranium goes from an ionization of 0.5 to roughly 0.9, but this will have little effect on the neutral hydrogen, except for perhaps polarization at close range. For this reason, the binary diffusion coefficient for hard sphere collisions will be maintained.

Electrical Conductivity

The success of the MHD enhancement depends upon establishing a current through the flow. If the current is assumed to consist mainly of electrons diffusing through the gas, the conductivity can be given by the expression [5]

$$\sigma = \frac{n_e e^2}{m_e \bar{\nu}_e} \tag{62}$$

where n_e is the electron number density. The collision frequency of the electrons with a species (j) is the product of their relative velocity, collision cross section, and number density of the species, or $\nu_{ej} = \bar{c}\sigma_{cj} n_j$. Summing over the species of ions and neutrals gives

$$\nu_e = \nu_{ei} + \bar{c} \sum_j \sigma_{cj} n_j \tag{63}$$

where σ_{cj} is taken as a constant for each neutral species over the applicable temperature range, n_j is found from the equilibrium relations discussed earlier, and ν_{ei} applies to all species of ions. If all quantities are expressed in mks units, ν_{ei} is given by [5]

$$\nu_{ei} = \frac{3.64(10^{-6}) n_i}{T^{3/2}} (16.38 + \tfrac{3}{2}\ell_n T - \tfrac{1}{2}\ell_n n_e) \tag{64}$$

Optical Gas Properties

In addition to the heat that is deposited in the solid regions of the core by neutrons and gamma rays, there is the possibility of significant heat transfer by black body radiation due to the high temperature of the gas. The propellant (hydrogen) has only one or two electrons, depending on whether it is in a monatomic or diatomic configuration. The radiation and emission spectra of these are discrete, with only a few transition lines present. At these few frequencies, the propellant flow appears opaque to electromagnetic (EM) radiation, but outside of these lines it is transparent. The uranium, however, has a very large number of electrons (92) and, with Doppler and thermal (collisional) broadening of the lines, gives the appearance of being optically active over a large continuum of energy levels. The degree to which the gas is "active" is made quantitative by introducing κ_ν.

If one looks at the intensity (as a function of frequency) of a beam of EM radiation traveling through a gas, its variation with distance is given by [11]

$$\frac{dI_\nu}{dx} = -\rho\kappa_\nu I_\nu + J_\nu \tag{65}$$

When the gas is in LTE, the emission and absorption coefficients are related by Kirchhoff's law:

$$\frac{J_\nu}{k_\nu} = \rho B_\nu \tag{66}$$

with B_ν, the Planck function, given by

$$B_\nu = \frac{2h\nu^3}{c^3} (\exp[h\nu/kT] - 1)^{-1} \tag{67}$$

Inserting Eq. (66) into Eq. (65) then gives

$$\frac{dI_\nu}{dx} = \rho\kappa_\nu [B_\nu - I_\nu] \tag{68}$$

This shows that the specific intensity increases along the path of the ray due to the excess of emission over absorption. Each of the terms in Eq. (68) has an implied spatial dependence, but explicit reference to this has been suppressed for brevity. Looking for a moment at just the absorption of radiation as it travels through the gas ($B_\nu = 0$), this equation can be integrated to the form $I_\nu = I_{\nu 0} e^{-\tau_\nu}$, where τ_ν is given by the expression

$$\tau_\nu = \int_0^x \rho\kappa_\nu \, dx' \tag{69}$$

The optical depth is a measure of the amount of absorbing (and radiating) matter in a given geometric length and is given in units of inverse length, usually cm^{-1}. The greater the value of τ_ν, the shorter the distance a beam of radiation will travel before losing a given amount of its energy.

From experimental work done by Parks, et al. [12], values of the opacity of a uranium gas over a large range of temperatures and pressures have been determined. Typical values of these opacities range from 10^3 to 10^4 cm/g. At uranium gas densities of 10^{-4} g/cm^3, the optical depth would have values on the order of 1 cm^{-1}, indicating that radiation generated at one point in the flow could travel 1 or 2 cm and still be carrying with it a significant portion of its energy. If the vortex tube is constructed to have a radius of a few centimeters or less, this would allow the high-temperature core radiation of the vortex to be transported to the walls, and the gas would be described as "optically thin."

A consequence of the desire for a low reactor mass is the high uranium loading discussed at the beginning of this paper. At pressures of hundreds of atmospheres and temperatures up to 10,000 K, the density of the uranium is around 1–10 kg/m^3 (10^{-3}–10^{-2} g/cm^3), making the optical depth of order 10–100 cm^{-1} over much of the uranium distribution. This implies most of the energy radiated away from a point will be deposited within 0.1 to 1 mm, which, assuming the same size of the vortex tube as before, makes the gas optically thick. This has a major impact on both the design and the analysis of this system. First, it indicates that to shield the outer walls of the vortex from the radiation generated at the core, the vortex radius should not be smaller than the centimeter range. The second impact comes from being able to model the radiative transfer of heat as a diffusive phenomenon, much like conduction.

Following the methodology of Taine [13], he shows that from the spectral intensity, the radiative heat flux at a point in the flow can be found in the form

$$\dot{q} = -\lambda_R(T) \frac{\partial T}{\partial x} \tag{70}$$

where the radiative conduction coefficient is given by

Appendix A

Table A1 Coefficients for the Gibbs function $\phi^\circ(T)$

Species	ϕ_0	ϕ	ϕ_{-2}	ϕ_{-1}	ϕ_1	ϕ_2	ϕ_3	$\Delta H_f^\circ(0)$
UF_1	1357.5050	41.7036	0.0147705	0.01009	9.7900	−2.619	0.139	-1.3×10^9
UF_2	502.2915	93.4560	−0.1261465	5.02597	−30.1598	6.189	−0.645	-5.62×10^5
UF_3	553.3866	98.2613	−0.0799027	3.71993	7.9759	−6.672	1.290	-1.06×10^6
UF_4	614.5832	124.8767	−0.1241181	5.96570	−0.6408	−3.016	0.684	-1.612×10^6
UF_5	713.6000	151.1544	−0.1173657	6.19798	−12.1199	1.589	−0.053	-1.893×10^6
UF_6	756.6497	157.9388	−0.0171950	3.09999	0.0507	−0.016	0.002	-2.141149×10^6
UF_1^+	359.8707	42.4549	0.0154827	0.02391	8.5809	−2.268	0.090	6.37×10^5
UF_2^+	461.4304	73.3237	−0.0772061	3.21915	7.9676	−6.670	1.290	9.8×10^4
UF_3^+	553.8460	100.7665	−0.1125839	4.50318	−3.4068	−1.908	0.501	-2.9×10^5
UF_4^+	612.3652	126.2158	−0.1149708	5.72262	−12.1267	1.591	−0.054	-5.62×10^5
UF_5^+	691.4709	133.0001	−0.0142656	2.49544	0.0444	−0.014	0.002	-8.78×10^5
UF_6^+	691.4709	133.0001	−0.0142656	2.49544	0.0444	−0.014	0.002	-8.78×10^5
UF_1^-	338.1402	37.4534	−0.0110581	0.66774	24.1559	−10.926	1.688	1.13×10^5
UF_2^-	463.6356	68.7893	0.0052763	1.19236	−2.9141	0.054	0.013	-6.62×10^5
UF_3^-	594.2478	118.3937	−0.1288438	5.76412	−30.1516	6.187	−0.645	-1.16×10^6
UF_4^-	616.2753	123.1922	−0.0847140	4.49984	7.9938	−6.678	1.291	-1.712×10^6
UF_5^-	717.9693	150.6358	−0.1197890	5.75842	−3.3818	−1.916	0.502	-2.118×10^6
UF_6^-	778.7786	176.0929	−0.1202938	6.80249	−12.1131	1.586	−0.053	-2.611×10^6
U	260.8313	39.6781	−0.1586499	4.95565	23.3505	−13.182	2.297	5.36×10^5
U^+	283.4652	40.9402	−0.0525755	2.44798	−16.2521	7.404	−1.442	1.133×10^6

$$\lambda_R(T) = \frac{4\pi}{3} \int_0^\infty \frac{1}{\rho_u \kappa_\nu} \frac{\mathrm{d}}{\mathrm{d}T} I_\nu^\circ[T(x)]\, \mathrm{d}\nu \tag{71}$$

Under the assumption of LTE, this can be given in a closed form as [14]

$$\lambda_R(T) = \frac{16\sigma T^3}{3\rho_u \kappa_R} \tag{72}$$

where κ_R has been tabulated [12] for various temperatures and pressures. Figure 4 shows the variation of the opacity as a function of temperature for several high pressures. The value of the Rosseland mean opacity (RMO) shows no pressure-dependence at temperatures less than 10,000 K, and above this is only slightly dependent over a large pressure range. The drop in RMO, as well as the dependence on pressure, can presumably be explained as a consequence of the uranium ionization, as it is the electron transitions that are responsible for the absorption and emission.

Conclusions

General partition functions were derived and explicitly calculated for hydrogen, fluorine, and electrons, and approximated for uranium fluorides via curve fitting of the Gibbs function. These partition functions were, in turn, used to calculate equilibrium concentrations of the various species present in different regions of the reactor. For uranium hexafluoride (UF_6) injection under load levels corresponding to a subcritical heating value at the outer wall, uranium condensation is not observed within the prescribed temperature range. Further, the dominant equilibrium species within the reactor are shown to be largely dependent on temperature; at higher temperatures, the hydrogen propellant increasingly interacts with the fuel to produce hydrogen fluoride (HF).

The ability to inject both fuel and propellant to the vortices within the same feed tubes was also determined. To avoid uranium condensation under the high pressures of the injection process, small amounts of fluorine can be introduced to reduce the partial pressure of the metallic uranium below the vapor pressure curve. This free fluorine cannot be sustained within the vortex and was therefore ignored in the equilibrium analysis.

Bulk transport properties such as the specific heat, electrical conductivity, and diffusion coefficients were also derived for the relevant species. The hard sphere interaction model was found to be a good approximation for both neutral and ionized species, the latter of which were shown to exhibit negligible Coulombic repulsion for temperatures as high as 10,000 K. Finally, optical properties of the gaseous U–F system were determined and, for an appropriate range of pressures and temperatures, the system was found to be optically thick. To shield the outer wall from electromagnetic radiation, the vortex tubes should be of radii no smaller than the centimeter range. Under such optically thick conditions, the dominant (radiative) heat transfer mode can be modeled as a diffusive phenomenon.

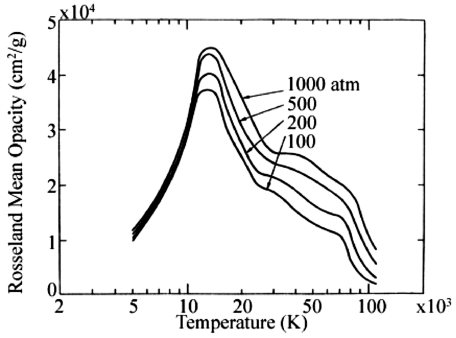

Fig. 4 Rosseland mean opacity vs temperature for a uranium plasma [12].

Acknowledgments

This research was funded in part by the Department of Defense through the Air Force Office of Scientific Research graduate research fellowship program and in part by the Massachusetts Institute of Technology, Department of Aeronautics and Astronautics. The authors would like to acknowledge Jack L. Kerrebrock for originating the concept and thank him for his significant support and guidance in its analysis.

References

[1] Sedwick, R. J., Zayas, D. A., and Kerrebrock, J. L., "Magneto-hydrodynamic Vortex Containment for Gas Core Nuclear Propulsion, Part 1: Concept Overview," *Journal of Propulsion and Power*, Vol. 23, No. 1, 2006, pp. 81–89.

[2] Kerrebrock, J. L., and Meghreblian, R. V., "Vortex Containment for the Gaseous-Fission Rocket," *Journal of the Aerospace Sciences*, Vol. 28, No. 9, 1961, pp. 710–24.

[3] Sedwick, R. J., "Analysis of an Open Cycle Gas Core Nuclear Propulsion System Using MHD Driven Vortices for Fuel Containment," Ph.D. Thesis, Dept. of Aeronautics and Astronautics, Massachusetts Inst. of Technology, Cambridge, MA, 1997.

[4] Sutton, G. P., *Rocket Propulsion Elements*, Wiley, New York, 1992.
[5] Mitchner, M., and Kruger, C. H., Jr., *Partially Ionized Gases*, Wiley, New York, 1992.
[6] Huang, Kerson, *Statistical Mechanics*, 2nd ed., Wiley, New York, 1987.
[7] Davidson, N., *Statistical Mechanics*, McGraw–Hill, New York, 1962.
[8] Anon., "CODATA Recommended Key Values for Thermodynamics." *Journal of Chemical Thermodynamics*, Vol. 10, No. 10, 1978, pp. 903–906.
[9] Gurvich, L. V., Yungman, V. S., Dorofeyeva, O. V., Gorokhov, L. N., and Munvez, S. S., "Thermodynamic Properties of Gaseous W-F and U-F Systems," *Proceedings of the Symposium on Thermophysical Properties*, American Society of Mechanical Engineers, New York, 1977, pp. 615–622.
[10] Chapman, S., and Cowling, T. G., *The Mathematical Theory of Non-Uniform Gases*, Cambridge Univ. Press, Cambridge, England, U.K., 1958.
[11] Penner, S. S., *Quantitative Molecular Spectroscopy and Gas Emissivities*, Addison–Wesley, Reading, MA, 1959.
[12] Parks, D. E., Lane, G., Stewart, J. C., and Peyton, S., "Optical Constants of Uranium Plasma," NASA CR-72348, GA-8244, Feb. 1968.
[13] Taine, J., and Petit, J. P., *Heat Transfer*, Prentice–Hall, Upper Saddle River, NJ, 1993.
[14] Seigel, R., and Howell, J. R., *Thermal Radiation Heat Transfer*, McGraw–Hill, New York, 1972.

G. Spanjers
Associate Editor